Journal of Solid State Chemistry **142,** 419–427 (1999)
Article ID jssc.1998.8057, available online at http://www.idealibrary.com on IDEAL®

Cation Deficiency in (Ba,Sr)$Co_{1-x}O_y$ Hexagonal Perovskite Related Oxides: New Members of the $A_{n+2}B'B_nO_{3n+3}$ Homologous Series

K. Boulahya, M. Parras, and J. M. González-Calbet[1]

Departamento de Química Inorgánica, Facultad de Químicas, Universidad Complutense, 28040-Madrid, Spain

Received June 8, 1998; in revised form October 5, 1998; accepted October 9, 1998

The new phases $(Ba_{0.5}Sr_{0.5})_7Co_6O_{18}$, $Ba_8Co_7O_{21}$, and $Ba_9Co_8O_{12}$ have been shown by electron diffraction and high-resolution electron microscopy to be three new members ($n = 5$, $n = 6$, and $n = 7$) of the 2H hexagonal perovskite-related $A_{n+2}B'B_nO_{3n+3}$ homologous series. Their modulated structures are made up of chains, running along the *c* direction and separated by Ba(Sr) ions, containing a succession of one Co atom in prismatic trigonal sites and *n* Co atoms in octahedral coordination sharing faces. The strategy to synthesize different terms of this family is discussed in terms of the distance between AO_3 layers. © 1999 Academic Press

Key Words: **homologous series $A_{n+2}B'B_nO_{3n+3}$, new Ba/Co ratio in; 2H related perovskites, cation deficiency in; Ba_3O_9 and Ba_3CoO_6 hexagonal stacking; electron diffraction and microscopy.**

INTRODUCTION

The ABO_3 perovskite structure is formed by the close packing of AO_3 layers leading to the formation of one BO_6 octahedron for every AO_3 unit. The hexagonal close packed stacking of these layers gives rise to the 2H polytype (1) which can be described as formed by isolated chains of octahedra sharing faces parallel to the *c* axis (Fig. 1a). Contradictory results on the structural features concerning anion deficient related 2H mixed oxides have been reported on several materials formulated as ABO_{3-y} (A = Ba, Sr; B = Co, Ni). In a series of recent papers, it has been established that these phases are, in fact, cation deficient with respect to the 2H perovskite hexagonal type. Actually, $BaNi_{0.83}O_{2.5}$ (2) is the same compound formerly formulated as 2H-$BaNiO_{2.67}$ (3) or $BaNiO_x$ (4), and the so called "low-temperature hexagonal form" 2H-$SrCoO_{2.5}$ (5) is isostructural with $BaNi_{0.83}O_{2.5}$ and must be correctly formulated as $SrCo_{0.83}O_{2.5}$ (6) or, most properly, as $A_6B_5O_{15}$ (A = Ba, Sr; B = Ni, Co).

[1] To whom correspondence should be addressed. Fax: 34 91 394 43 52. E-mail: jgcalbet@eucmax.sim.ucm.es.

Although the stacking sequence of these grossly cation deficient hexagonal perovskite related phases preserves the hexagonal symmetry, it consists of mixed layers A_3O_9 and $A_3A'O_6$, the latter resulting from the former by substitution of three oxygen atoms by one A' atom. This sequence leads to a structure made up of chains parallel to the *c* axis, separated by *A* atoms and formed by a trigonal prismatic site occupied by A' cations which are linked, in $A_6B_5O_{15}$, to four BO_6 octahedra sharing faces. This structure is related to that shown by Sr_4PtO_6 (7), which is made up of chains parallel to the *c* axis, separated by strontium atoms (Fig. 1b). Within the chains, PtO_6 octahedra are linked by common faces to triangular prisms occupied by strontium atoms (A'). More recently, an isostructural compound with $A' = B$, $Ca_3Co_2O_6$, has been reported (8).

All these oxides exhibit either trigonal or rhombohedral cell with an *a* parameter between 0.9 and 1.0 nm and differ from one another by the value of the *c* parameter, which corresponds to the stacking direction of the octahedra and prisms. According to Darriet and Subramanian (9), this family of compounds, resulting from the stacking of mixed A_3O_9 and $A_3A'O_6$ layers, can be represented by the general formula $A_{3n+3}A'_nB_{n+3}O_{6n+9}$, all the members having either trigonal or rhombohedral symmetry. $n = 0$ corresponds to the ABO_3 perovskite, whereas the $n = \infty$ and $n = 1$ terms correspond to the Sr_4PtO_6-type structure and $A_6B_5O_{15}$ (A = Ba, Sr; B = Ni, Co), respectively. More recently, two slightly different $n = 1$ members of this family have been described for $Ba_6MIr_4O_{15}$ (10). When M = Cu, the $n = 1$ member is obtained with ordered distribution of Ir and Cu in both A' and B sites. When M = Zn, a related incommensurate structure is observed. The first example of an $n = 2$ phase has been reported by Campá *et al.* (11) for $Sr_9Ni_{6.64}O_{21}$, with some vacancies in prismatic sites. An $n = 3$ phase $Sr_{12}Ni_{7.5}O_{27}$, in which half of the trigonal prismatic sites are occupied by Ni^{4+}, has been described by Strunk and Müller-Buschbaum (12).

Abraham *et al.* (13) have isolated another vacancy-free polytype related to the 2H hexagonal type, whose structure has been recently studied by electron diffraction

0022-4596/99 $30.00

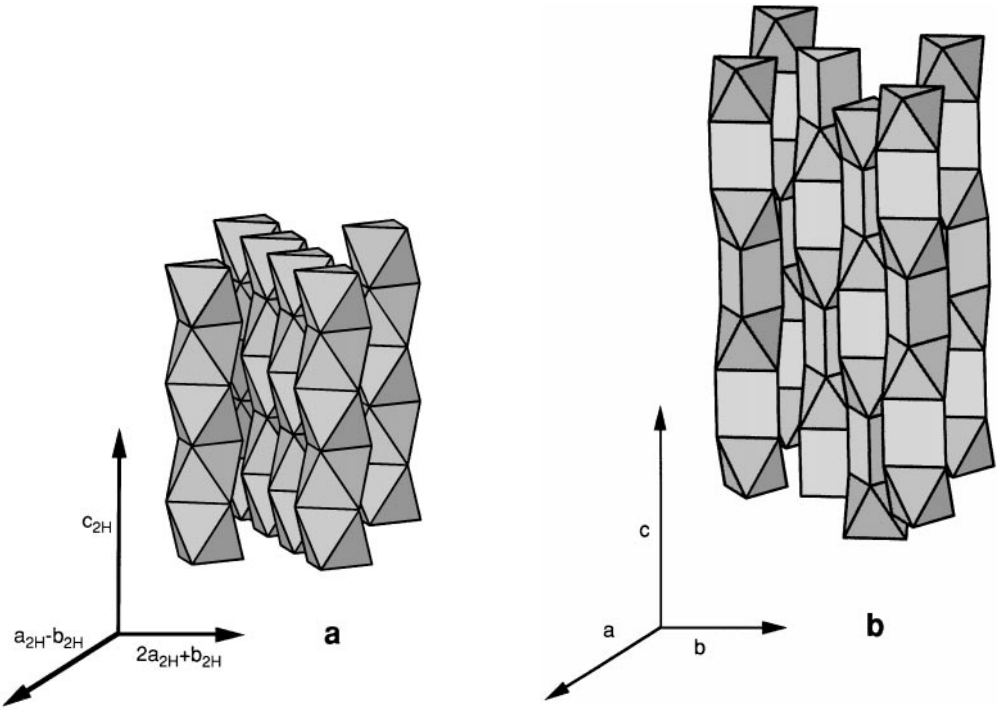

FIG. 1. (a) Schematic representation of the 2H-ABO_3 structure. (b) Schematic representation of the $Ca_3Co_2O_6$ structure.

and microscopy by Huvé *et al.* (14). $Sr_4Ni_3O_9$ can also be described as consisting of chains, separated by strontium ions, of two NiO_6 octahedra and one Ni face-sharing trigonal prism. According to these authors, this oxide corresponds to the $m = 2$ member of a series of the general formula $A_n(B_mC_l)O_x$, where n is the number of Ba or Sr ions between the chains per cell, m is the number of successive B ions in octahedral coordination, and l is the number of successive prisms along the c direction. No evidence has been found for the ocurrence of successive face-sharing prisms; therefore, the l value is always 1. On the basis of this formulation, Sr_4PtO_6 is the $m = 1$ member, whereas $Sr_4Ru_2O_9$ (15), corresponding to $m = 2$, is made up of chains containing a succession of an empty prism and two octahedra, and $A_6B_5O_{15}$ is the $m = 4$ term of this family.

According to the composition expressed by the formula $A_{3n+3}A'_nB_{n+3}O_{6n+9}$, none of the cation defficient phases with $B/A > 0.83$ could exist. In fact, all the results reported thus for phases with $B/A \leq 0.83$, which puts the limit to four octahedra and one trigonal prism per row. Since the 2H type, formed by ∞ octahedra, is stable, it has been our objective to look for new members of this series between them. We describe in this paper the structural models of three new members with a ratio $B/A > 0.83$ in the Ba(Sr)–Co–O system, as deduced by selected area electron diffraction (SAED) and high-resolution electron microscopy (HREM).

EXPERIMENTAL

$Ba_9Co_8O_{24}$ and $Ba_8Co_7O_{21}$ were prepared by heating in air stoichiometric amounts of $BaCO_3$ and Co_3O_4 at 920°C for 5 days. $(Ba_{0.5}Sr)_7Co_6O_{18}$ was obtained when stoichiometric amounts of the corresponding Ba and Sr carbonates and Co oxide were treated in air at 900°C for 72 h. The average cationic composition was established by inductive coupling plasma (ICP), while the local composition in every crystal was determined by energy dispersive spectroscopy (EDS). For this purpose, a JEOL scanning electron microscope JSM-8600 equipped with an energy-dispersive system LINK AN10000 was employed. The oxygen content was determined, within $\pm 1 \times 10^{-2}$, from the cobalt average oxidation state analyzed by titration with Mohr's salt. All results are consistent with the $Ba_9Co_8O_{24}$ and $Ba_8Co_7O_{21}$ compositions.

Powder X-ray diffraction (XRD) was carried out on a SIEMENS D-5000 diffractometer using Cu$K\alpha$ radiation. SAED was performed on a JEOL 2000FX electron microscope, fitted with a double tilting goniometer stage ($\pm 45°$). HREM was carried out on a JEOL 4000EX electron microscope, fitted with a double tilting goniometer stage ($\pm 25°$),

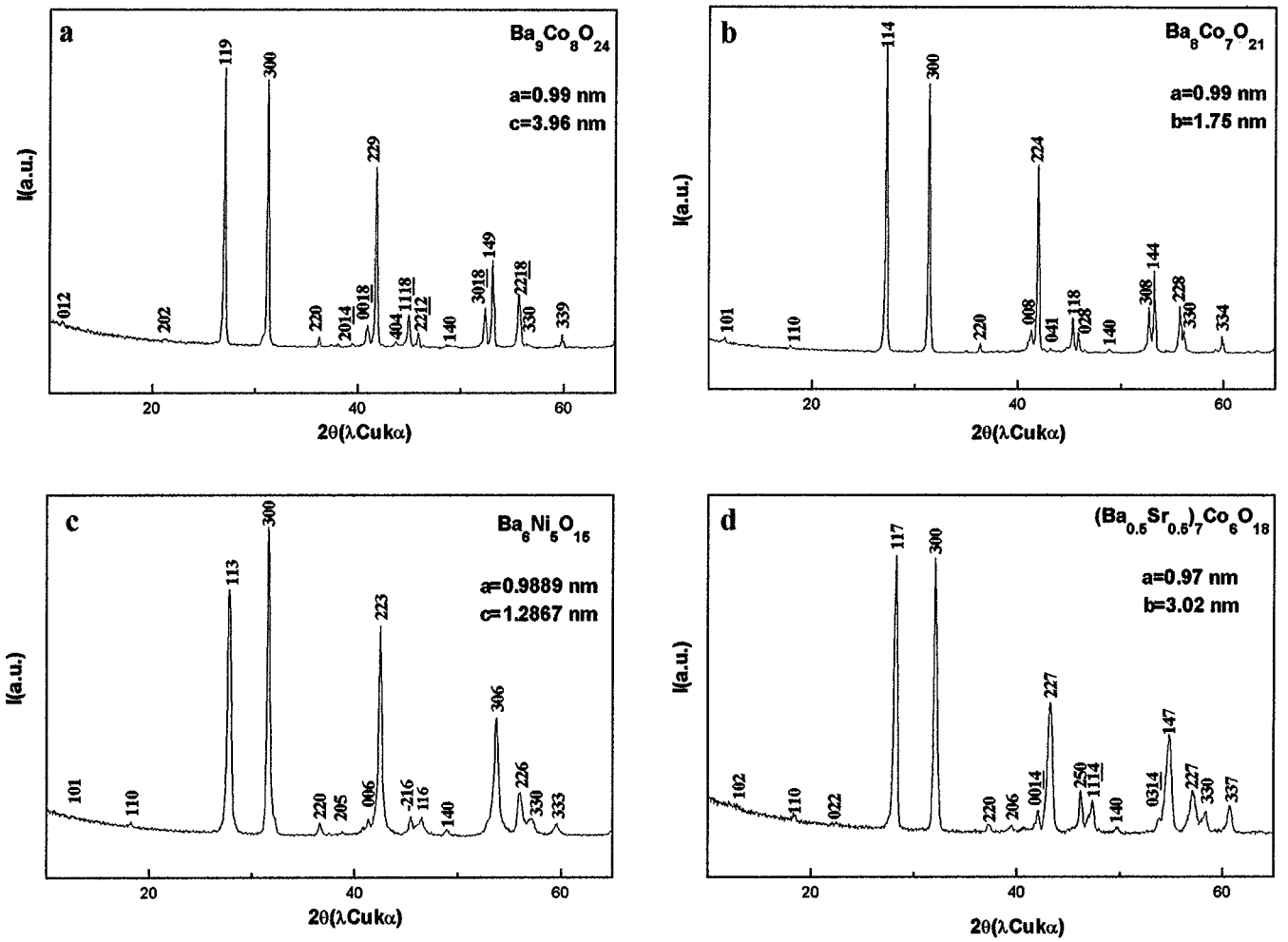

FIG. 2. XRD patterns corresponding to (a) $Ba_9Co_8O_{24}$, (b) $Ba_8Co_7O_{21}$, (c) $Ba_6Ni_5O_{15}$, and (d) $(Ba_{0.5}Sr_{0.5})_7Co_6O_{18}$.

by working at 400 kV. Samples were ultrasonically dispersed in *n*-butanol and transferred to carbon-coated copper grids.

RESULTS AND DISCUSSION

The powder XRD patterns corresponding to $Ba_9Co_8O_{24}$ (Fig. 2a) and $Ba_8Co_7O_{21}$ (Fig. 2b) are very similar to the pattern shown by $Ba_6Ni_5O_{15}$ (9) (Fig. 2c). All reflections can be indexed on the basis of a rhombohedral unit cell, with an *a* parameter close to 0.98 nm. Even though the compositions are quite different, the XRD patterns look similar, which makes it difficult to elucidate the structure. Therefore, it is essential to use SAED to explain the stacking sequence of octahedra and trigonal prismatic units along *c* axis more clearly.

Figure 3a shows the SAED pattern along $[1\bar{1}0]_{2H}$ corresponding to $Ba_6Ni_5O_{15}$ (subindex 2H refers to the 2H basic cell). A commensurate modulated sixfold superlattice along $[222]^*_{2H}$ is apparent which can be indexed, according to X-ray data previously reported (2), on the basis of a unit cell with parameters $a = 0.9889$ nm and $c = 1.2867$ nm, S.G. *R*32. The SAED pattern along the same projection corresponding to $Ba_9Co_8O_{24}$ (Fig. 3b) shows a commensurate modulated structure, corresponding to a ninefold superlattice along $[332]^*_{2H}$, which could be assigned to a rhombohedral cell with parameters $a = 0.990$ and $c = 3.96$ nm, and $R\bar{3}c$ as a possible space group.

Figure 3c shows the SAED pattern corresponding to $Ba_8Co_7O_{21}$ along $[1\bar{1}0]_{2H}$. Although this pattern seems to be more complex, the general characteristics are similar to those observed in Figs. 3a and 3b. This material shows a commensurate modulated 24-fold superstructure along $[886]^*_{2H}$. Although in this pattern, satellite reflections up to the fourth order are observed, some superstructure spots are not seen due to the high superlattice order. A trigonal cell

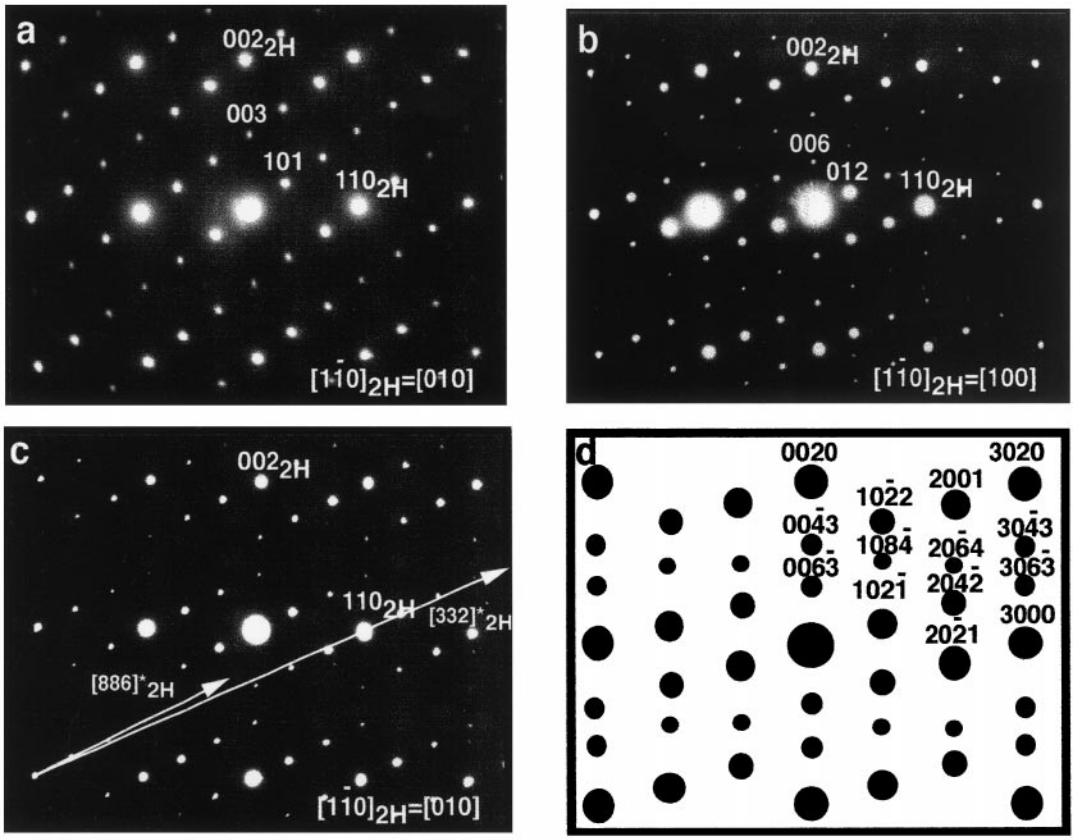

FIG. 3. SAED patterns along $[1\bar{1}0]_{2H}$ corresponding to (a) $Ba_6Ni_5O_{15}$, (b) $Ba_9Co_8O_{24}$, and (c) $Ba_8Co_7O_{21}$, (d) schematic representation showing the four indices necessary to simultaneously describe both the hexagonal and rhombohedral subsystems in $Ba_8Co_7O_{21}$.

with parameters $a = 0.999$ nm and $c = 1.75$ nm, S.G. $P321$, can be proposed.

Such a modulation can be a consequence of the interaction between two subsystems, as proposed by Ukei *et al.* (16) for $Ba_x(Pt,Cu)O_3$. The first subsystem corresponds to Ba sublattice with trigonal symmetry and similar parameters in all cases ($a \approx 0.570$ nm; $c \approx 0.438$ nm), whereas the second corresponds to Co sublattice and presents a rombohedral lattice with a unit vector given for $Ba_6Ni_5O_{15}$, by $q = (a^*_h + b^*_h)/3 + 1.66c^*_h \approx 0.72$ nm, a^*_h, b^*_h and c^*_h referring to the hexagonal sublattice. Hexagonal axes $a^* = (a^*_h + b^*_h)/3$, $b^* = (2b^*_h - a^*_h)/3$, and $c^* = 1.66c^*_h$ are adopted for the rombohedral system to describe simultaneously both sublattices for a unique pattern. For $Ba_9Co_8O_{24}$ the unit vector is $q = (a^*_h + b^*_h)/3 + 1.77c^*_h \approx 0.78$ nm and for $Ba_8Co_7O_{21}$ the unit vector is $q = (a^*_h + b^*_h)/3 + 1.75c^*_h \approx 0.76$ nm. To index such patterns, a set of four indices h, k, l, and m corresponding to a^*_h, b^*_h, c^*_h and c^* are needed, as schematically shown in Fig. 3d for $Ba_8Co_7O_{21}$. The order of satellite reflections, caused by the interaction between the two subsystems, is expressed by means of ($|l|$) and ($|m|$). Thus, ($hkl0$) and ($hk0m$) refer to the main reflections, while ($hkl1$), ($|l| > 0$) and ($hk1m$), ($|m| > 0$) are the first order satellites, ($hkl2$), ($|l| > 1$) and ($hkm2$), ($|m| > 1$) are second order satellites, etc. Satellite reflections of, at least, third and fourth order are seen. For this reason, all spots are seen in 6- and 9-fold superstructures, as in the case of $Ba_6Ni_5O_{15}$ and $Ba_9Co_8O_{24}$, but not in the 24-fold superlattice corresponding to $Ba_8Co_7O_{21}$.

Figure 4 shows the $Ba_9Co_8O_{24}$ high-resolution image along $[1\bar{1}0]_{2H}$. An apparently well-ordered material is observed with d-spacings 1.98 and 0.86 nm, corresponding to d_{002} and d_{100} of the unit cell described above for this material. For a better understanding of the contrast observed in this image, a comparison with the same projection in $Ba_6Ni_5O_{15}$ can be useful. The $Ba_6Ni_5O_{15}$ high-resolution image along $[1\bar{1}0]_{2H}$ (Fig. 5) shows a sequence of bright dots of different contrast which can be associated to nickel columns formed by one prism and four octahedra sharing faces along the c axis. The two brightest dots in this sequence probably correspond to Ni prisms along $[\bar{1}01]$ equivalent to $[\bar{3}\bar{3}3]_{2H}$. Such a stacking sequence along the c axis corresponds to an ordered intergrowth of Ba_3NiO_6 and Ba_3O_9 layers.

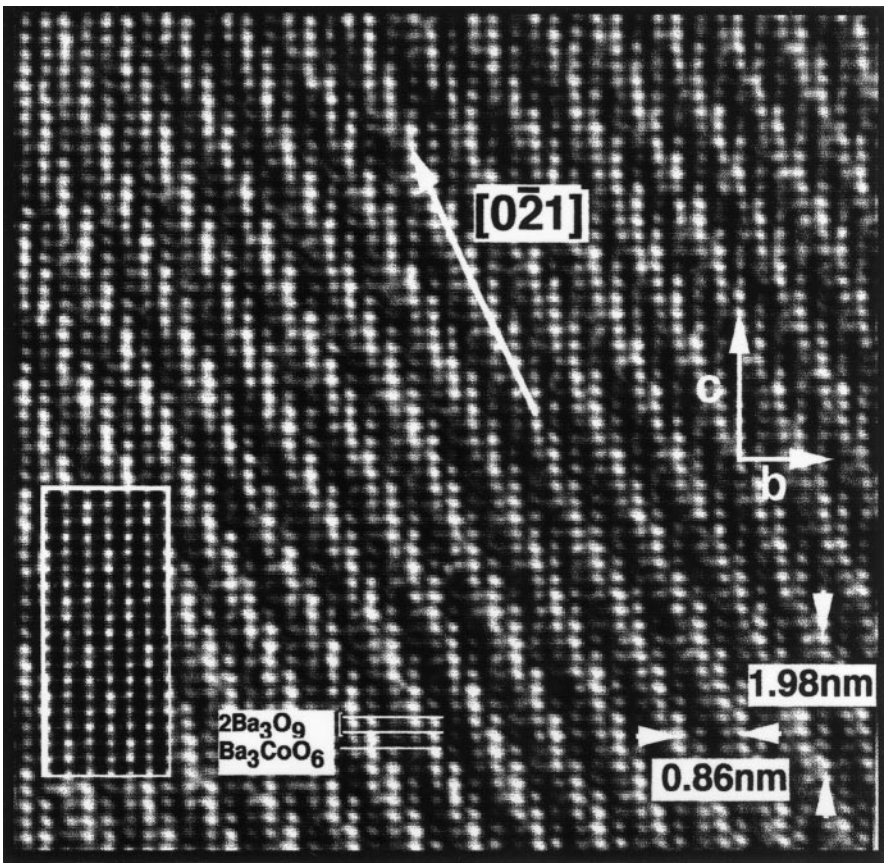

FIG. 4. HREM corresponding to $Ba_9Co_8O_{24}$ along $[1\bar{1}0]_{2H}$. The calculated image is shown in the inset. Bright dots are aligned along $[0\bar{2}1]$.

Similarly, the contrast variation observed in the $Ba_9Co_8O_{24}$ image can be interpreted as being due to the ordered intergrowth of a trigonal prism and seven octahedra sharing faces along the *c* axis. In this case, the Co prisms are aligned along $[0\bar{2}1]$, which, in this case, is equivalent to $[\bar{6}\bar{6}9]_{2H}$, the previous sequence corresponding to an alternation of two Ba_3O_9 layers and one Ba_3CoO_6 layer along the *c* axis.

The contrast variation in the $Ba_8Co_7O_{21}$ high-resolution image (Fig. 6) can be interpreted as being due to the ordered intergrowth along the *c* axis of one trigonal prism and six octahedra sharing faces, as a consequence of an ordered stacking sequence of two (2 Ba_3O_9/Ba_3CoO_6) layers and one (Ba_3O_9/Ba_3CoO_6) layer along the *c* axis.

Figure 7 shows the structural models corresponding to the 6:5, 8:7, and 9:8 phases along $[1\bar{1}0]_{2H}$. It can be seen that the main difference between these structures is the number of octahedra along the *c* axis. The 8:7 phase introduces two more octahedra along *c* than 6:5 and the 9:8 material one more than 8:7. On the basis of these results, it seems plausible to predict the existence of a 7:6 phase in this series. However, the synthesis of a material with the composition $Ba_7Co_6O_{18}$ was not suscessful, since a mixture phase was always obtained, $Ba_8Co_7O_{21}$ being by far the majority phase. Moreover, the $Ba_6Co_5O_{15}$ composition could not be isolated. But, 6:5 is stable in Co-2H related perovskites with Sr in *A* positions (6). This is reflected in the decrease of 0.01 nm of the *c* axis for $Ba_9Co_8O_{24}$ ($c_{2H} = 0.45$ nm) and $Ba_8Co_7O_{21}$ ($c_{2H} = 0.44$ nm), i.e., when the ratio Ba/Co increases. This shows that to stabilize a higher concentration of *B* cationic vacancies, keeping $B = Co$ same, we have to reduce the size of the metals in the *A* positions, i.e., the distance between AO_3 layers.

According to that, we have partially substituted Ba by Sr to isolate a material with the composition $(Ba,Sr)_7Co_6O_{18}$. A monophasic material is obtained for Ba:Sr = 0.5:0.5. The SAED pattern and corresponding HREM image along $[1\bar{1}0]_{2H}$ are shown in Fig. 8. As can be observed, a commensurate modulation with $q = 0.701$ nm appears, leading to a trigonal cell with parameters $a = 0.97$ nm, $c = 3.02$ nm. Taking into account that the c^* component of *q* vector corresponds to $(2c^*_{2H} - (1/7)2c^*_{2H})$, the first satellite is located at $(1/3\ 1/3\ 1/7)_{2H}$; therefore, this phase can be described as a modulated 21-fold superstructure along $[776]^*_{2H}$.

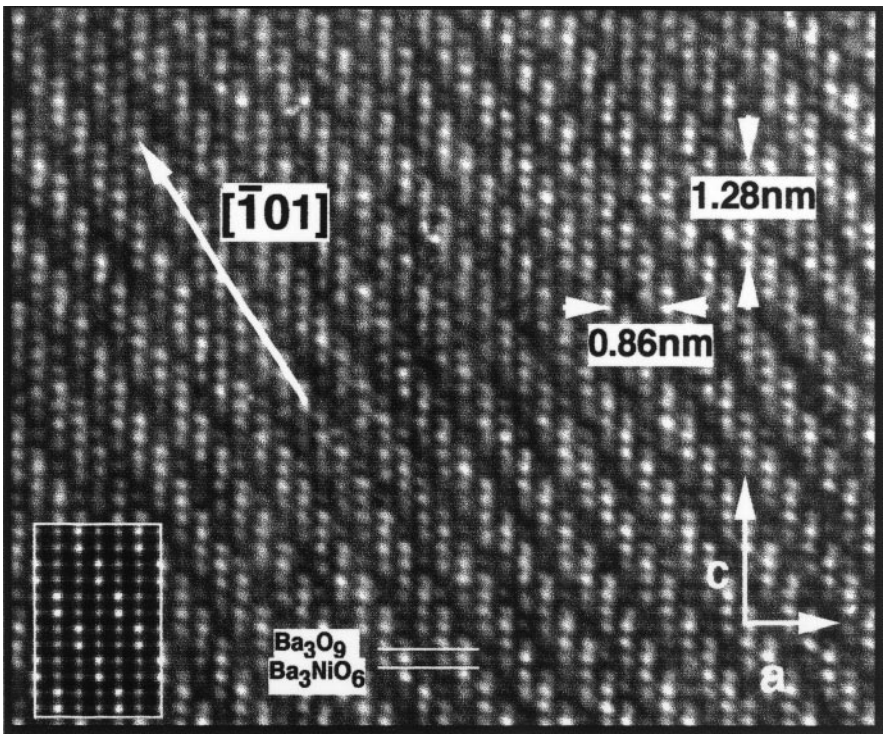

FIG. 5. HREM corresponding to $Ba_6Ni_5O_{15}$ along $[1\bar{1}0]_{2H}$. The calculated image is shown in the inset. Bright dots are aligned along $[\bar{1}01]$.

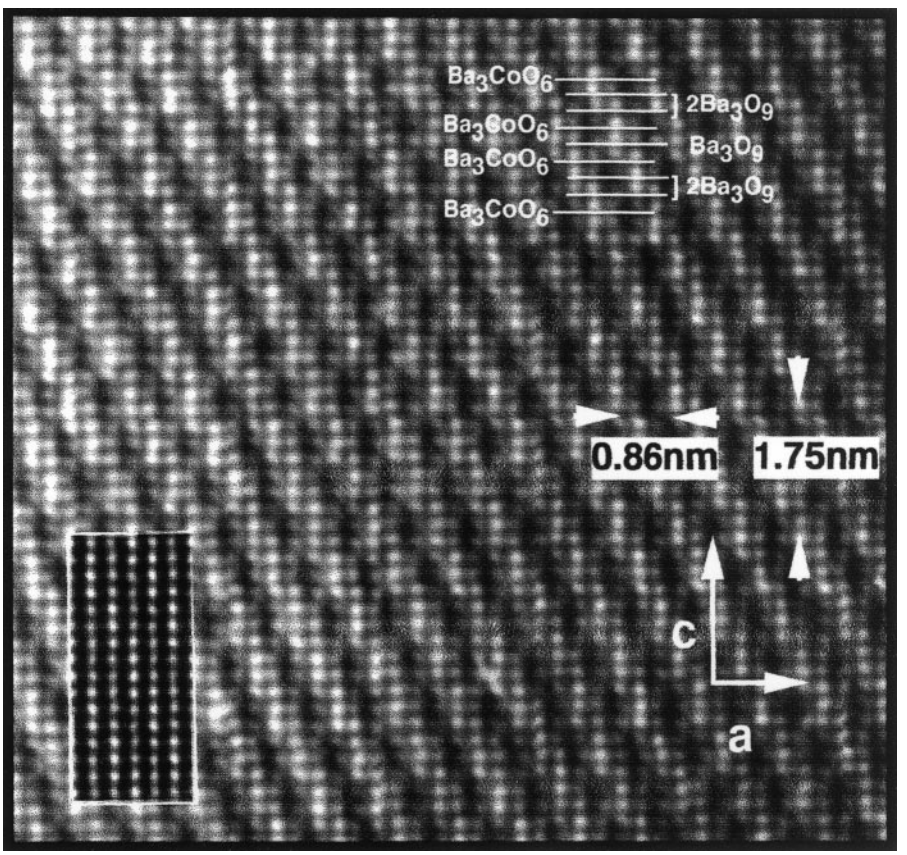

FIG. 6. HREM corresponding to $Ba_8Co_7O_{21}$ along $[1\bar{1}0]_{2H}$. The calculated image is shown in the inset.

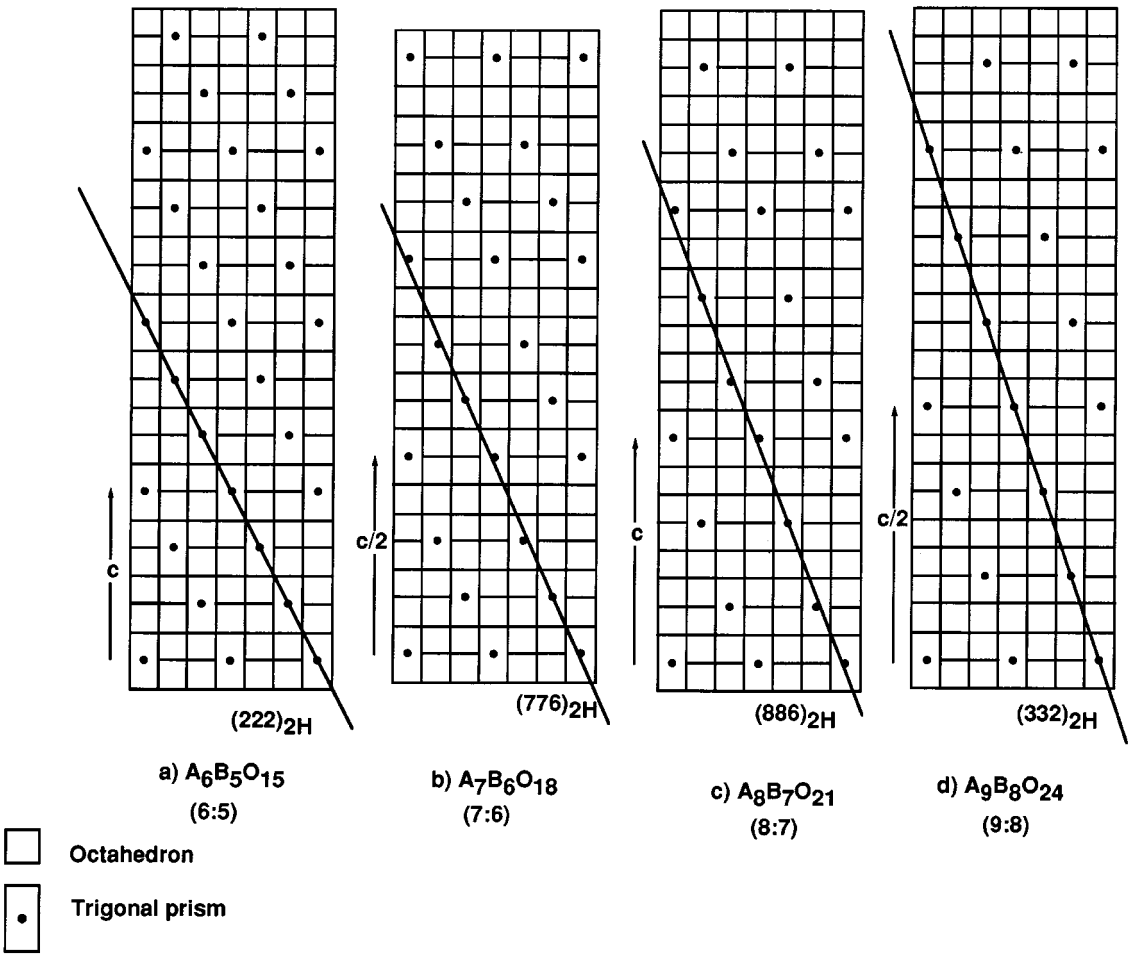

FIG. 7. Idealized representation of (a) 6:5, (b) 7:6 (c) 8:7, and (d) 9:8 structural models along $[1\bar{1}0]_{2H}$. Planes $(222)_{2H}$, $(776)_{2H}$, $(886)_{2H}$, and $(332)_{2H}$ are outlined.

Although satellite reflections up to the fourth order are observed, some superstructure spots are not seen due to the high order of the superlattice. The contrast variation observed in the HREM image of $(Sr_{0.5}Ba_{0.5})_7Co_6O_{18}$ can be interpreted as being due to an ordered intergrowth of a trigonal prism and five octahedra sharing faces along c axis, i.e., as corresponding to an ordered stacking sequence of three (A_3O_9/A_3CoO_6) layers and one $(2A_3O_9/A_3CoO_6)$ layer along the c axis (A = Sr, Ba). As expected, the structural model of the 7:6 phase introduces one more octahedra along the c axis than the 6:5 composition, as shown in Fig. 7. Also we have been successful in preparing a composition $(Sr_{0.75}Ba_{0.25})_6Co_5O_{15}$ which is isostructural with $Ba_6Ni_5O_{15}$ and $Sr_6Co_5O_{15}$.

The interpretation of the image contrast in the HREM images obtained has also been made with the help of a simulation program using the Mac Tempas package. Image calculations were carried out under the following image conditions: sample thickness between 3.0 and 8.0 nm, $\Delta f = -97.5$ to -70 nm, $C_s = 1.0$ mm, beam divergence angle $= 0.7 \times 10^{-3}$ rad, and accelerating voltage = 400 kV. A good fit with the experimental images along $[110]_{2H}$ is obtained for the following conditions:

— $Ba_6Ni_5O_{15}$: $\Delta f = -90$ and sample thickness of 5.0 nm (inset to Fig. 5).

— $(Sr_{0.5}Ba_{0.5})_7Co_6O_{18}$: $\Delta f = -90$ and sample thickness of 7.0 nm. (inset to Fig. 8).

— $Ba_8Co_7O_{21}$: $\Delta f = -90$ and sample thickness of 7.0 nm (inset to Fig. 6).

— $Ba_9Co_8O_{24}$: $\Delta f = -90$ and sample thickness of 5.0 nm (inset to Fig. 4).

The comparison between the structural models indicates that the 9:8 phase can be derived from the 6:5 material by the addition of one and one-half frames of the 2H phase parallel to the c axis, both keeping rhombohedral symmetry as deduced from the corresponding SAED patterns. In the same way, the 7:6 phase can be derived from the 6:5 material by the introduction of only a half-frame of the 2H phase, but

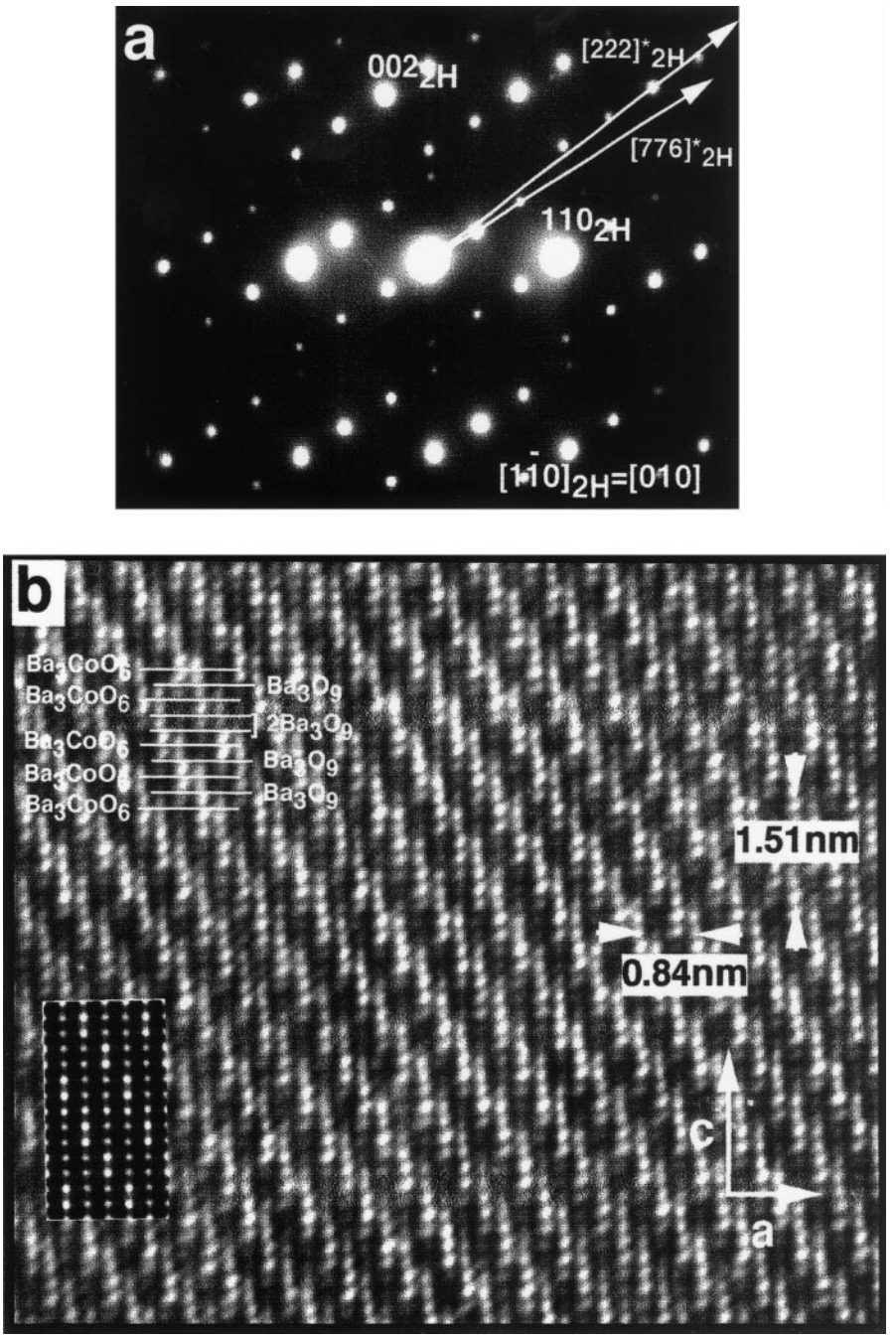

FIG. 8. (a) SAED pattern and (b) HREM corresponding to $(Ba_{0.5}Sr_{0.5})_7Co_6O_{18}$ along $[1\bar{1}0]_{2H}$. The calculated image is shown in the inset.

if this half-frame is removed from the 9:8 phase, the 8:7 composition is obtained. Both effects originate a displacement of the Co prisms from (1/3 2/3) along the *a* cell axis and (2/3 1/3) along the *c* cell axis, breaking the rhombohedral symmetry in 7:6 and 8:7 materials, as observed in the corresponding SAED patterns.

As a consequence, the Co atoms in prism coordination are located every six $(222)_{2H}$ planes in $Ba_6Ni_5O_{15}$, in such a way that they are aligned following the $[\bar{3}\bar{3}3]_{2H}$ direction. In $Ba_9Co_8O_{24}$, since there are three more octahedra along the *c* axis, such prisms can be found for every nine $(332)_{2H}$ planes following the $[\bar{6}\bar{6}9]_{2H}$ direction, leading to the different superlattices observed in the corresponding SAED patterns. The situation is slightly different for $A_7Co_6O_{18}$ (A = Ba, Sr) and $Ba_8Co_7O_{21}$ since the Co prisms are not aligned along the cell diagonal because only every third

alternating unit is along a 2H plane. In the former, the Co prisms can be found in three successive $(776)_{2H}$ planes for every 21 units and, in the latter, in three successive $(886)_{2H}$ planes for every 24 units, leading to the modulated superstructures seen in the SAED patterns. This misalignment of the trigonal prisms along the cell diagonal in the 8:7 phase can be considered as an "orientation" anomaly along the $[332]^*_{2H}$ direction. Such an anomaly has been used by Ye and Amelinckx (17) when the sequences of satellites have directions which enclose a small angle with the directions of the rows of spots due to the basic sublattice (as arrowed in Fig. 3c). The structure is then no longer rhombohedral. The same effect is observed in the 7:6 phase, which can be considered as an orientation anomaly along $[222]^*_{2H}$ (as seen in Fig. 8a).

The structural characteristics of these new materials are analogous to that shown by the terms of the $A_{3n+3}A'_nB_{n+3}O_{6n+9}$ homologous series, since all of them can be described as being due to the ordered alternation of Ba_3CoO_6 and Ba_3O_9 layers. However, 9:8, 8:7, and 7:6 compounds cannot strictly be considered members of this family. Every term of the mentioned series is defined as being formed by one A_3O_9 layer inserted after every n $A_3A'O_6$ layers. As a consequence of such a definition, there can be no other formulation between $A_6B_5O_{15}$ and stoichiometric 2H-ABO_3. In fact, this series cannot include a composition with a B/A ratio higher than 0.83, i.e., the phases formed by a number of A_3O_9 layers higher than the number of $A_3A'O_6$ layers. As a consequence, the 9:8, 8:7, and 7:6 ratios cannot be described from the general formula $A_{3n+3}A'_nB_{n+3}O_{6n+9}$.

However, these phases can be described considering the insertion of an $A_3A'O_6$ layer for every n A_3O_9 layers, as terms of a family with the composition $A_{3n+3}A'B_{3n+1}O_{9n+6}$. Now, the $n = 0$ term should only consist of $A_3A'O_6$ layers and the $n = \infty$ term should correspond to the 2H type. The $n = 1$ term, as in the previous series, should be formed by one A_3O_9 layer and another $A_3A'O_6$ layer, i.e., $A_6B_5O_{15}$ ($A' = B$). The $n = 2$ term should be formulated as $A_9B_8O_{24}$, and the successive terms should have a higher proportion of A_3O_9 layers, showing a lower deviation of the 1:1 cationic ratio, corresponding to $n = \infty$. However, with such a general formula it is not possible to include materials with cationic ratio $B/A < 5/6$, except the 3:2 phases which correspond to the $n = 0$ term.

On the contrary, all these phases can be formulated in a general way as proposed by Huvé *et al.* (14) with the composition $A_n(B_mC_l)O_x$. However, such a description gives no information of the structural components and the relationship between each term. An alternative way to describe this homologous series is by means of the expression $A_{n+2}B_nB'O_{3n+3}$, where n is an integer which denotes the number of B cations with octahedral coordination parallel to the c axis and B' refers to one B cation in trigonal prism coordination. Moreover, this general formula allows us to determine directly the superstructure reciprocal direction with respect to the 2H subcell, which can be expressed by means of $[(n + 2)\ (n + 2)\ 6]^*_{2H}$.The $n = 1$ term of this series is $Ca_3Co_2O_6$, $Sr_4Ni_3O_9$ and $Sr_4CuIr_2O_9$ being $n = 2$ terms (18), $A_6B_5O_{15}$ is the $n = 4$ member and $n = 5$, 6, and 7 are the new terms reported in this paper, with $[776]^*_{2H}$, $[886]^*_{2H}$, and $[996]^*_{2H}$ superstructure reciprocal directions, respectively.

ACKNOWLEDGMENT

We acknowledge the finantial support of CICYT (Spain) through Research Project MAT95-0642.

REFERENCES

1. J. J. Lander, *Acta Crystallogr.* **4,** 148 (1951).
2. J. A. Campá, E. Gutierrez Puebla, M. A. Monge, I. Rasines, and C. Ruiz-Valero, *J. Solid State Chem.* **108,** 230 (1994).
3. H. Krischner, K. Torkar, and B. O. Kolbesen, *J. Solid State Chem.* **3,** 349 (1971).
4. Y. Takeda, F. Kanamaru, M. Shimada, and M. Koizumi, *Acta Crystallogr. B* **32,** 2464 (1976).
5. J. C. Grenier, S. Ghodbane, and G. Demazeau, *Mater. Res. Bull.* **21,** 429 (1986).
6. W. T. A. Harrison, S. L. Hegwood, and A. Jacobson, *J. Chem. Soc. Chem. Commun.*, 1953 (1995).
7. J. J. Randall and L. Katz, *Acta Crystallogr.* **12,** 519 (1959).
8. H. Fjellvag, E. Gulbrandsen, S. Aasland, A. Olsen, and B. C. Hauback, *J. Solid State Chem.* **124,** 190 (1996).
9. J. Darriet and M. A. Subramanian, *J. Mater. Chem.* **5,** 543 (1995).
10. P. D. Battle, G. R. Blaque, J. Darriet, J. G. Gore, and F. Weill, *J. Mater. Chem.* **7,** 1559 (1997).
11. J. Campá, E. Gutiérrez-Puebla, A. Monge, I. Rasines, and C. Ruiz-Valero, *J. Solid State Chem.* **126,** 27 (1996).
12. M. Strunk and H. Müller-Buschbaum, *J. Alloys Comp.* **209,** 189 (1994).
13. F. Abraham, S. Minaud, and C. Renard, *J. Mater. Chem.* **4,** 1763 (1994).
14. M. Huvé, C. Renard, F. Abraham, G. Van Tendeloo, and S. Amelinckx, *J. Solid State Chem.* **135,** 1 (1998).
15. C. Dusarrat, J. Fompeyrine, and J. Darriet, *Eur. J. Solid State Inorg. Chem.* **32,** 3 (1995).
16. K. Ukei, A. Yamamoto, Y. Watanabe, T. Shishido, and T. Fukuda, *Acta Crystallogr. B* **49,** 67 (1993).
17. H. Q. Ye and S. Amelinckx, *J. Solid State Chem.* **61,** 8 (1986).
18. P. D. Battle, G. R. Blake, J. Sloan, and J. F. Vente, *J. Solid State Chem.* **136,** 103 (1998).